ORIGINAL ARTICLE

Controlling the physical parameters of crystalline CIGS nanowires for use in superstrate configuration using vapor phase epitaxy

Dongjin Lee[1] · H. C. Jeon[1] · T. W. Kang[2] · Sunil Kumar[2]

Abstract

Indium tin oxide (ITO) is a suitable candidate for smart windows and bifacial semi-transparent solar cell applications. In this study, highly crystalline $CuInGaSe_2$ (CIGS) nanowires were successfully grown by horizontal-type vapor phase epitaxy on an ITO substrate. Length, diameter, and density of the nanowires were studied by varying the growth temperature (500, 520, and 560 °C), time (3.5, 6.5, and 9.5 h), and type of catalyst (In, Au, and Ga). Length, diameter, and density of the nanowires were found to be highly dependent on the growth conditions. At an optimized growth period and temperature of 3.5 h and 520 °C, respectively, the length and diameter of the nanowires were found to increase when grown in a catalyst-free environment. However, the density of the nanowires was found to be higher while using a catalyst during growth. Even in a catalyst-free environment, an Indium cluster formed at the bottom of the nanowires. The source of these nanowires is believed to be Indium from the ITO substrate which was observed in the EDS measurement. TEM-based EDS and line EDS indicated that the nanowires are made up of CIGS material with a very low Gallium content. XRD measurements also show the appearance of wurtzite CIS nanowires grown on ITO in addition to the chalcopyrite phase. PL spectroscopy was done to see the near-band-edge emission for finding band-to-band optical transition in this material. Optical response of the CIGS nanowire network was also studied to see the photovoltaic effect. This work creates opportunities for making real solar cell devices in superstrate configuration.

Keywords CIGS nanowires · Length · Diameter · Density · Vapor phase epitaxy · ITO

Introduction

For smart windows and bifacial solar cell applications, $CuInGaSe_2$ (CIGS) thin films directly grown on indium tin oxide (ITO) are low in efficiency due to the poor grain morphology at the CIGS/ITO interface. Commercial CIGS solar cells with Mo as the substrate are the best in terms of efficiency but are still useless for these kinds of applications due to its opacity. Also, CIGS thin films are unable to have solar cells with a large surface area for a higher photon absorption. In order to solve these problems, one-dimensional (1D) nanostructures could be considered and

have many advantages for photovoltaic applications (McEvoy et al. 2012; Stelzner et al. 2008; Garnett et al. 2008; Ho et al. 2012). The nanowires have potential advantages over planar wafer-based or thin-film solar cells in almost every step of the photo-conversion process. These include large surface-to-volume ratio for enhancing the external quantum efficiency (QE), enhanced light trapping by the reduction of Fresnel reflection, band gap tuning, facile strain relaxation, increased defect tolerance, and carrier flow restriction in the desired direction (Liu et al. 2011; Mehta et al. 2005). These benefits are not expected to enhance the maximum efficiency above a certain limit. Nonetheless, nanowires can reduce the quantity and quality of material necessary to reach those limits, allowing appreciable cost reductions in comparison to thin films. Nanowires provide us with the opportunities to fabricate single-crystalline semiconductor devices directly on low-cost substrates such as aluminum foil, stainless steel, and conductive glass, addressing another major cost-related issue to photovoltaic technology. In general, 1D nanostructures grow in single-crystalline form and

✉ Sunil Kumar
    sunilkumar32@gmail.com

[1] Quantum Functional Semiconductor Research Center, Dongguk University-Seoul, Jung-Gu, Seoul 100715, South Korea

[2] Nano Information Technology Academy, Dongguk University-Seoul, Jung-Gu, Seoul 100715, South Korea

have many advantages over thin films but it is difficult to grow highly crystalline nanowires with a desired density and a minimum number of defects on a desired substrate.

CIGS is I–III–VI compound semiconductor and is used to make a p-type layer in commercial thin-film solar cell technology. The optical band gap energy varies from 1.04 eV (CIS) ~ 1.67 eV (CGS). Advantages of CIGS include a high absorption coefficient and the highest conversion efficiency in thin-film solar cells. A variety of methods such as post-process in polycrystalline CIGS layer (Liu et al. 2011), formation of ZnO/CdS QD/CIS nanocrystal structure (Zhang et al. 2012), diffusion of Cu in Cu pad by annealing after growing In_2Se_3 nanowires (Cui et al. 2007), and the use of an anodic alumina membrane to grow nanowires (Wagner and Ellis 1964) were used for fabricating different kinds of CIGS nanostructures. Research on CIGS 1D nanostructures is undergoing but until now CIGS nanowires have only been grown on sapphire substrates because of the orientation relationship between CIGS and the sapphire substrate (Lee et al. 2015). However, these methods are unable to fabricate highly single-crystalline CIGS 1D nanostructures with a minimum number of defects on a transparent electrode. It is always desirable to grow crystalline CIGS nanowires on a fully transparent substrate like ITO. Very few researchers have tried to grow CIGS thin films on ITO-coated glass for smart windows and bifacial solar cell applications (Moon et al. 2014; Chu et al. 2014). To the best of our knowledge, no one has tried to grow CIGS nanowires on a transparent ITO. On a transparent substrate like ITO, researchers are unable to fabricate highly crystalline CIGS nanowires with the right composition, few number of defects, and are unable to align the nanowires with a controlled length, diameter, and density. In this work, CIGS nanowires are fabricated by optimizing the vapor phase epitaxy (VPE) method. The effects of temperature, growth time, and type of catalyst used were studied to obtain highly crystalline CIGS nanowires with a desired length, diameter, and density.

Experimental details

CIGS nanowires were deposited on an ITO-coated (Corning 7059) substrate by the VPE method. A schematic diagram of the Vapor Phase Epitaxy setup is shown in Fig. 1a. The ampoule containing the CIGS melted source is shown in Fig. 1b. The argon gas pressure was controlled to attain an ambient gas environment. Vaporized sources were Copper (Cu, 99.9995%, Sigma-Aldrich), Indium (In, 99.999%, Sigma-Aldrich), Gallium (Ga, 99.9999%, Alpha-Aesar), and Selenium (Se, 99.999%, Sigma-Aldrich). These sources had already been melted to achieve an educed mixed state. To find the optimized growth conditions, growth temperatures were varied from 500 to 560 °C. The temperature of the last
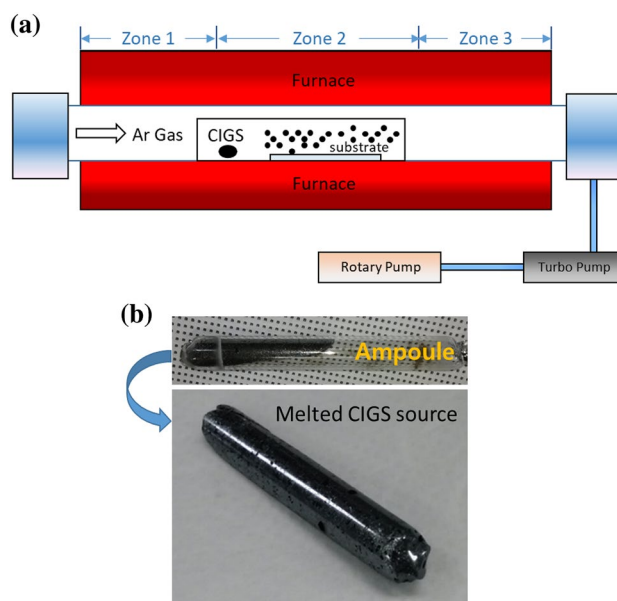

Fig. 1 a Setup of vapor phase epitaxy (VPE) and **b** melted CIGS source

zone was kept lower than 100 °C compared to the first and second zones. A quartz tube was heated for 30 min, then cooled for 30 min. The growth time was varied from 3.5 to 9.5 h to identify the optimal growth rate. The results were characterized by a scanning electron microscope (SEM), energy-dispersive spectrometer (EDS), transmission electron microscope (TEM), high-resolution TEM (HR-TEM), Line EDS, PL (photoluminescence), and optical response.

Results and discussion

Figure 2 shows the SEM images of top and cross-sectional views of CIGS nanowires grown for 3.5 h at temperatures of 500, 520, 540, and 560 °C. Length, diameter, and density of the CIGS nanowires were studied by varying the temperature within a fixed time for optimizing growth conditions for a certain temperature. The length, diameter, and density of the nanowires slightly increase when the temperature increases from 500 to 520 °C (Fig. 2a, c). Nanowires grown at 540 °C (Fig. 2e) show that the density of the nanowires rapidly decreases compared to growth at 520 °C, whereas length and diameter sharply increase. This can be due to the reason that the nanowires start merging into bigger nanowires at higher temperatures because atoms gain enough energy at higher temperatures and start to diffuse on the surface and form bigger nanowires with lower density. Samples grown at 560 °C (Fig. 2g) do not produce any nanowires. The sample grown at 520 °C was found to have the highest quality
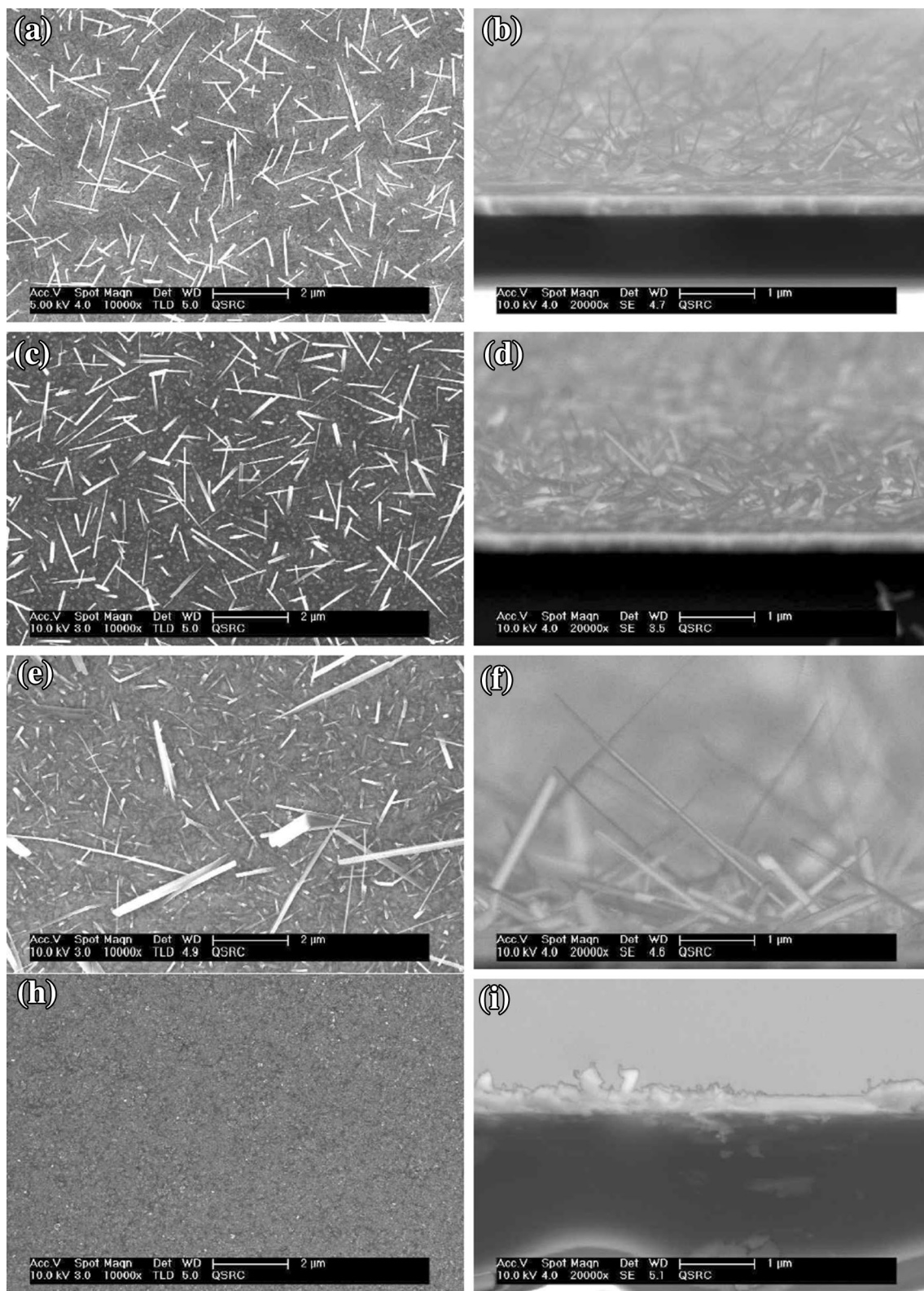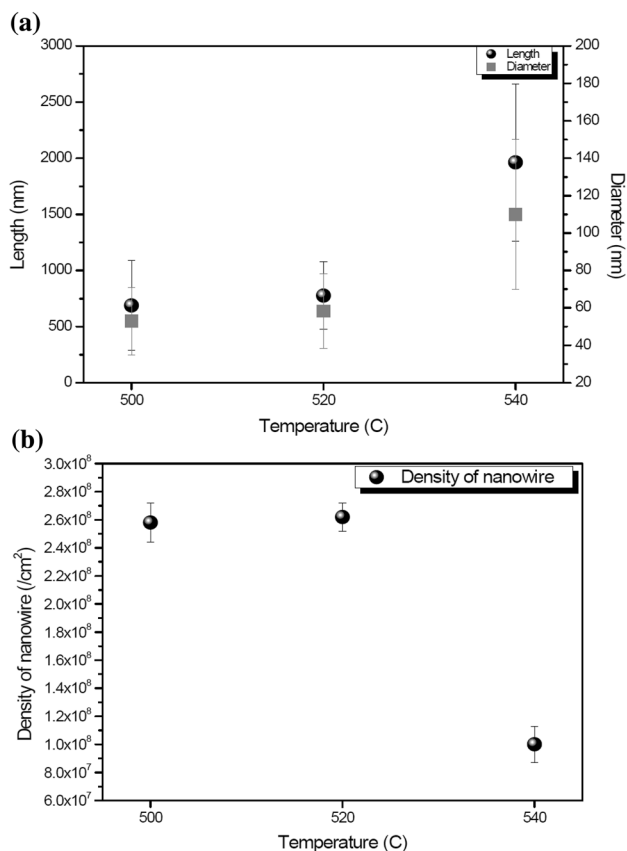
Fig. 2 SEM images of CIGS nanowire grown at temperature of **a**, **b** 500 °C; **c**, **d** 520 °C; **e**, **f** 540 °C; **g**, **h** 560 °C. **a**, **c**, **e**, and **g** are top view; **b**, **d**, **f**, and **h** are cross-section view

of nanowires in terms of length, diameter, and density. Although the sample grown at 520 °C produced smaller nanowires than the sample grown at 540 °C (Fig. 3a), the density of the nanowires is higher than other samples. (Figure 3b). Solar cells require a large surface area, and denser nanowires have a higher surface area than nanowires with big size alone. In order to optimize the CIGS nanowire growth rate, the growth time was varied from 3.5 to 9.5 h, while the temperature was held constant at 520 °C. Figure 4 shows the corresponding SEM images. The average length and diameter of the nanowires increase from ~ 780 to 1610 nm and from 58 to 80 nm, respectively (Fig. 5a, b). In the first 3.5 h, the growth rate is approximately 220 nm/h, but in next 6 h, the growth rate decreased to about 140 nm/h. A cluster-type formation can be seen at the bottom of all the nanowires (Fig. 6a). This cluster was characterized by Energy-Dispersive X-ray Spectroscopy (EDS) in SEM mode. The result is shown in Fig. 6b. From the EDS results, we came to know that the cluster contains Indium and Oxygen. The source and carrier gas do not contain Oxygen. This confirms that the bottom cluster is naturally oxidized and only Indium is present. Just to confirm the role of Indium

for the growth of CIGS nanowires, Indium, Gallium, and Gold were used as different catalysts, respectively. Samples were deposited at 520 °C during 3.5 h. Figure 7 shows the CIGS nanowires grown on different catalysts. CIGS nanowires grew only when using Indium as a catalyst. When Gold was used as a catalyst, only clusters are visible. When Gallium was used, only the ITO surface was visible. This confirms that only Indium can function as a catalyst for growing CIGS nanostructures. The mechanism of how the CIGS nanowires were grown by VPE method can be explained by the vapor–liquid–solid (VLS) mechanism. During the VLS mechanism (Wagner and Ellis 1964; Cheyssac et al. 2006; Huang et al. 2001), the source vapor reacts with the metal particles, which acts as a catalyst, and forms alloy droplets. After reaching the supersaturation state, the grown droplets lead to the formation of nanostructures. A typical characteristic of the VLS mechanism is the presence of metal particles capped at the end of the grown nanostructures. Because the melting point of Indium is 156.60 °C at 760 Torr, the Indium layer melted and formed liquid droplets. The liquid droplets acted as catalyst to the CIGS nanowires. Gallium also has a low melting point (29.78 °C at 760 Torr). Nevertheless, CIGS nanowires could not be grown while using Gallium as a catalyst. It could be possible that Indium from the ITO substrate helps Indium to uniformly cover the substrate. Then Indium acts as a catalyst for CIGS nanowires which was not the case when using Gallium and Gold. Figure 8a, b shows the length, diameter, and density of the CIGS nanowires grown on a non-catalyst and on an Indium catalyst substrate. This result shows that nanowires grown with Indium as a catalyst are more in number but with a smaller size. This means Indium can act effectively for the growth of CIGS nanowires.

The crystalline structure of the optimized CIGS nanowires grown at 520 °C for 3.5 h was investigated by TEM measurement in normal and high-resolution mode. Figure 9a shows a low-magnification TEM image. Figure 9b is a high-resolution TEM (HR-TEM) image. The formation of CIGS nanowires was also confirmed by EDS line scan in TEM mode. Figure 10a, b, and Table 1 show the Line EDS, EDS spectra, and the corresponding composition of the nanowires, respectively. From the graphs and the table, it appears that large quantities of Cu were present in the CIGS nanowires. This is because a copper grid was used to measure TEM. It was found that Cu, In, Se, and a small amount of Ga co-exist in the nanowires. XRD studies were also conducted to understand the morphology and it shows mixed CIGS phases composed of wurtzite and chalcopyrite structures, as shown in Fig. 11. The chalcopyrite structure matches well with the (JCPDS card no. 35-1101) and (JCPDS card no. 85-1575). The appearance of wurtzite phase is in addition to the earlier studies on CIGS nanowires

Fig. 3 a Effect of growth temperature on length and diameter of nanowires. b Effect of growth temperature on density of nanowires
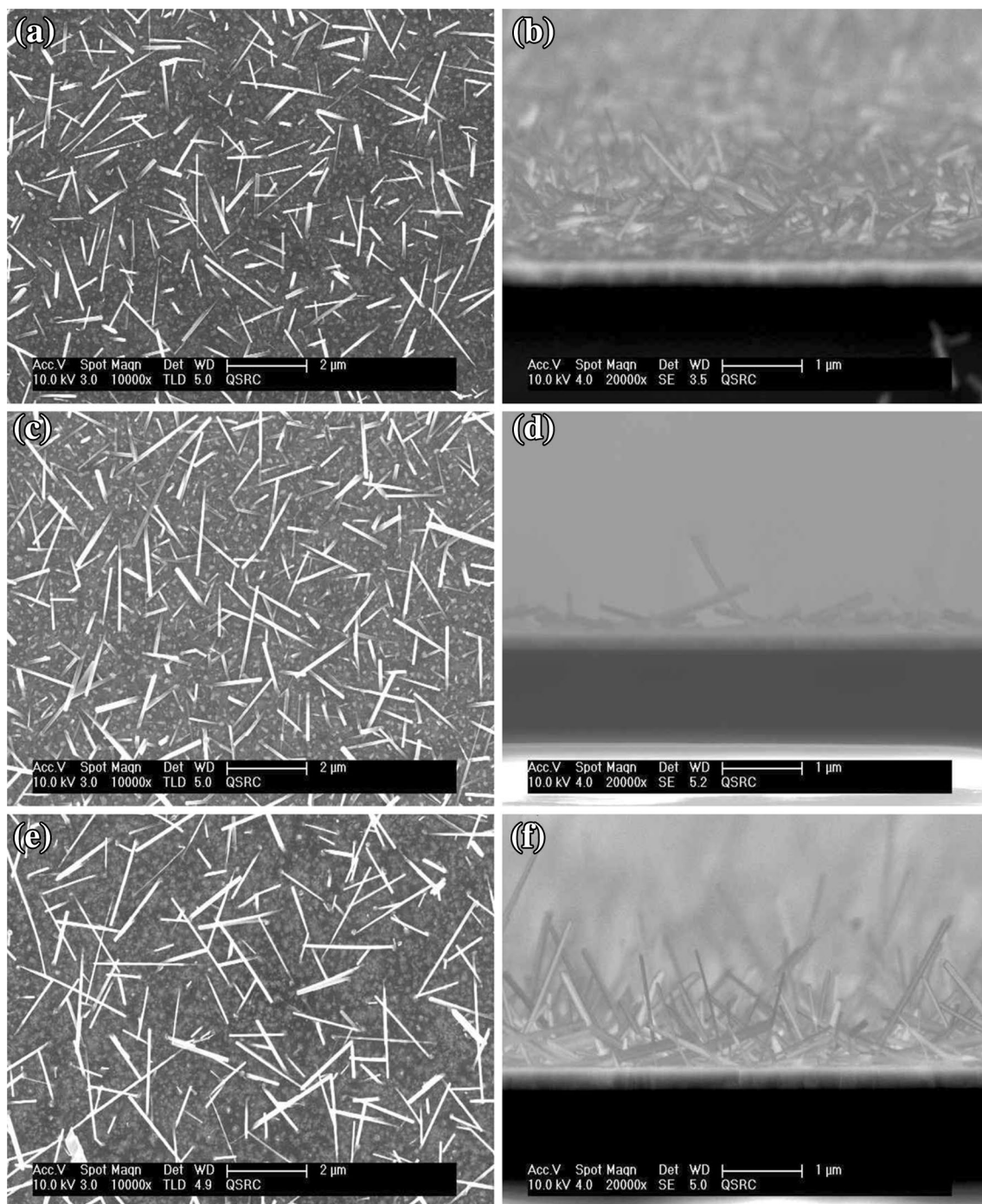
Fig. 4 SEM images of CIGS nanowires with various growth time; **a**, **b** 3.5 h; **c**, **d** 6.5 h; **e**, **f** 9.5 h. Growth temperature of these samples is 520 °C

which have shown the formation of only chalcopyrite structure (Wada et al. 2001). As wurtzite phase is not available in the existing JCPDS files, the wurtzite phase was matched as per the simulations done in one of the earlier studies (Norako and Brutchey 2010).

To identify the band gap energy of the optimized CIGS nanowires grown at 520 °C for 3.5 h, energy-resolved

photoluminescence measurement (PL) was used. A He–Ne laser (6328 Å) was used as an excitation source. The PL was measured at room temperature. The peak energy of PL spectrum was calculated by Gaussian fitting. Figure 12 shows the result of PL spectrum and Gaussian fitting. The dominant PL peak at 1.16 eV is the near-band-edge (NBE) emission mainly due to the band-to-band transition. The weak PL
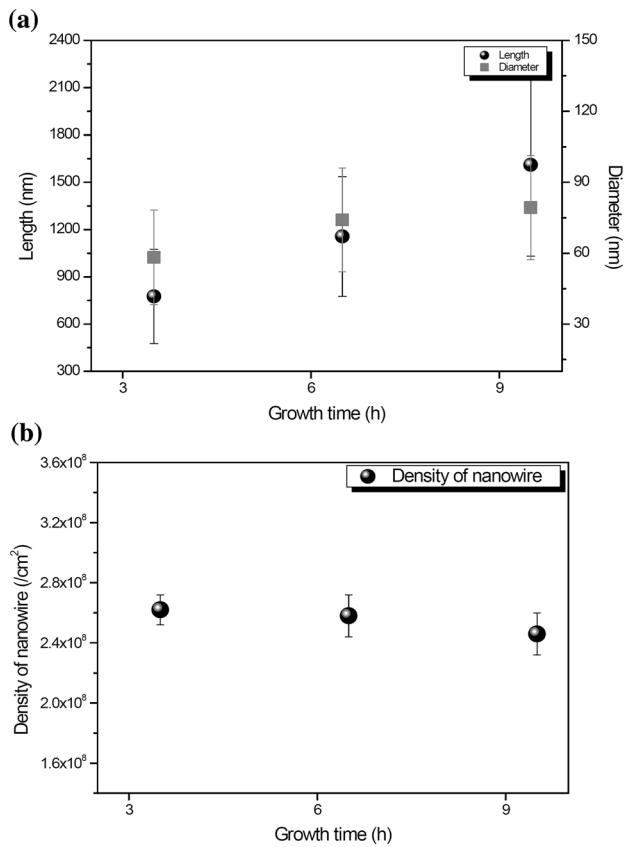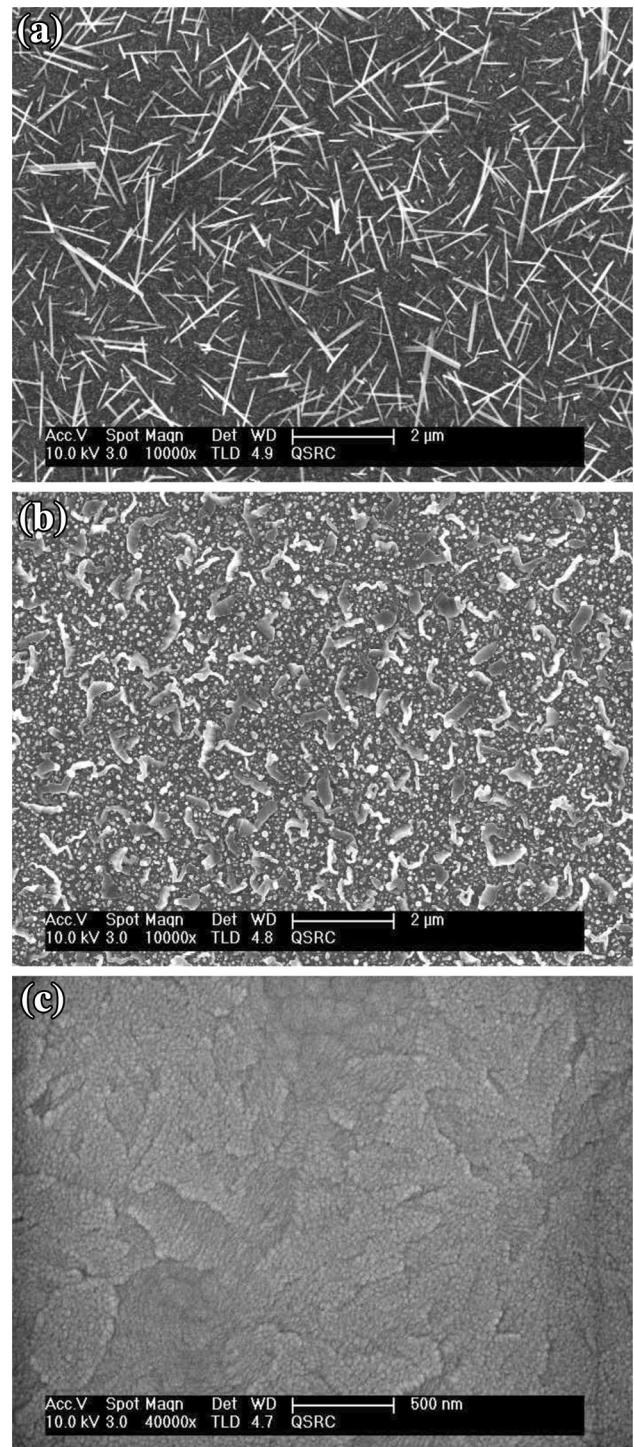
Fig. 5 **a** Length and diameter of nanowire by changing growth time. **b** Density of nanowire by changing growth time
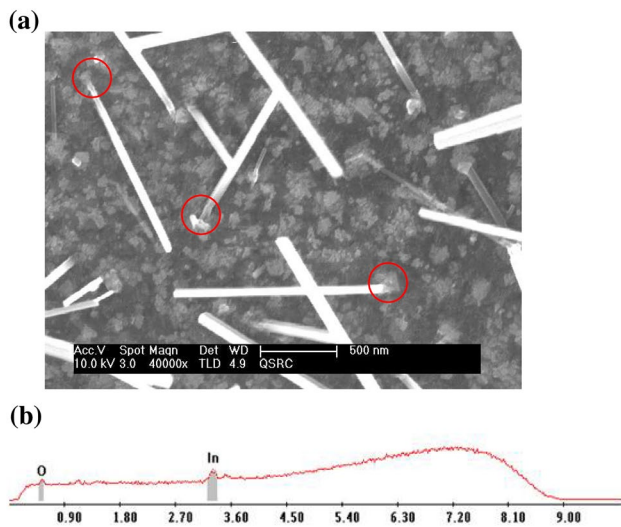

Fig. 6 **a** SEM image of root of CIGS nanowire. **b** EDS graph of root of CIGS nanowire

peak at 1.08 eV observed for the CIGS film may be due to the native defect such as Se vacancy (depth of 80 meV) (Shirakata et al. 2011, 2012).

Fig. 7 SEM images of CIGS nanowires with various catalyst; **a** In, **b** Au, and **c** Ga. Growth condition of these samples is same at 520 °C, 3.5 h

To confirm the photovoltaic effect of the optimized CIGS nanowires, the optical response of the CIGS nanowire network was measured. A nanowire network was made by dipping CIGS nanowires in ethanol and then were sonicated
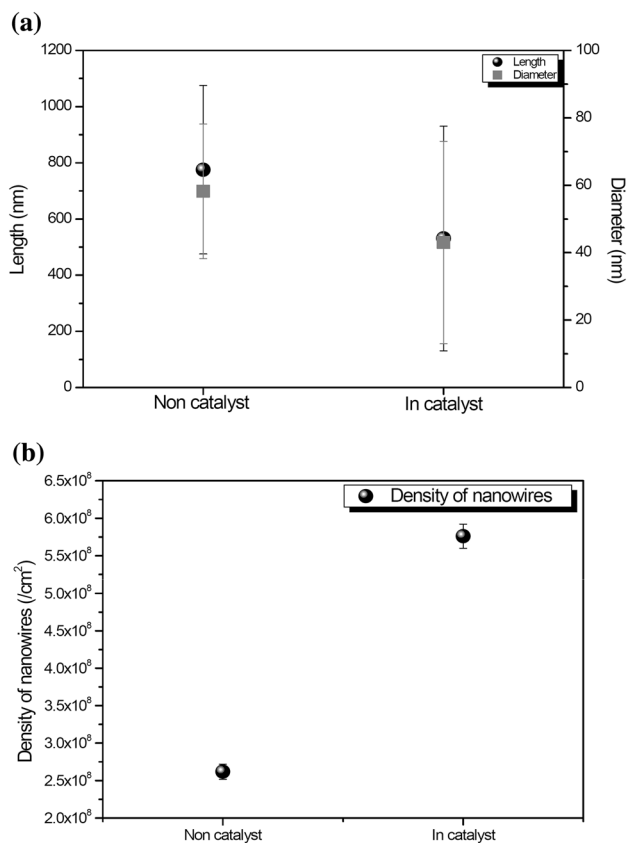
Fig. 8 a Length and diameter of nanowires with and without catalyst. **b** Density of nanowires with and without catalyst

to prepare well-dispersed CIGS nanowire suspensions (Heo et al. 2008). Then the CIGS nanowires and ethanol solution were dropped between Cu electrode pads. Figure 13a shows a schematic image of the CIGS nanowire network. Optical response was measured using a Keithley 617 Programmable Electrometer which was used to measure current signal between the Cu pads. Light exposure from a 20-W fluorescent lamp was given to the CIGS nanowire network periodically. Figure 13b shows the optical response of the CIGS nanowire network. When the lamp was turned on and light was exposed to the nanowire network, the photo current rapidly increased. When the lamp was turned off, the photo current sharply decreased. Even if the photo current response value is small, by this measurement, one can imagine the photovoltaic effect of CIGS nanowires-based pn junction in a real device.

Conclusions

Highly crystalline CIGS nanowires were grown directly on an ITO substrate by horizontal-type VPE method. Nanowires were grown by changing the growth temperature, growth
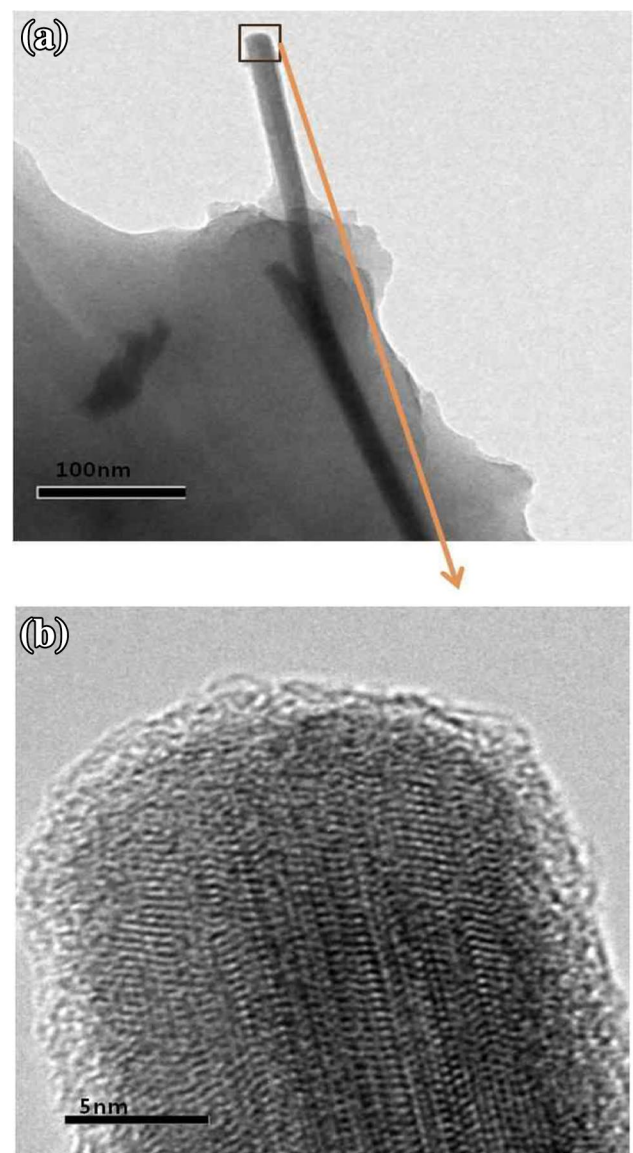
Fig. 9 a Low-magnification TEM image and **b** HR-TEM image

time, and the type of catalyst used. Their length, diameter, and densities varied as a result. At the fixed growth time of 3.5 h in a catalyst-free environment, and when the temperature increases from 500 to 540 °C, the length and diameter of the nanowires increase. The density of the nanowires increases up to 520 °C, then sharply decreases at 540 °C. At 560 °C, a CIGS film is grown on the substrate instead of nanowires. The growth rate was also studied by varying the growth time from 3.5 to 9.5 h at a fixed temperature of 520 °C. The length and diameter increase but the density decreases with the increase in time. It was found that even in a non-catalyst environment, only Indium can catalyze the growth of nanowires. This is because the source of Indium in CIGS was vaporized due to the low melting point. As a result, the CIGS nanowires were grown on the
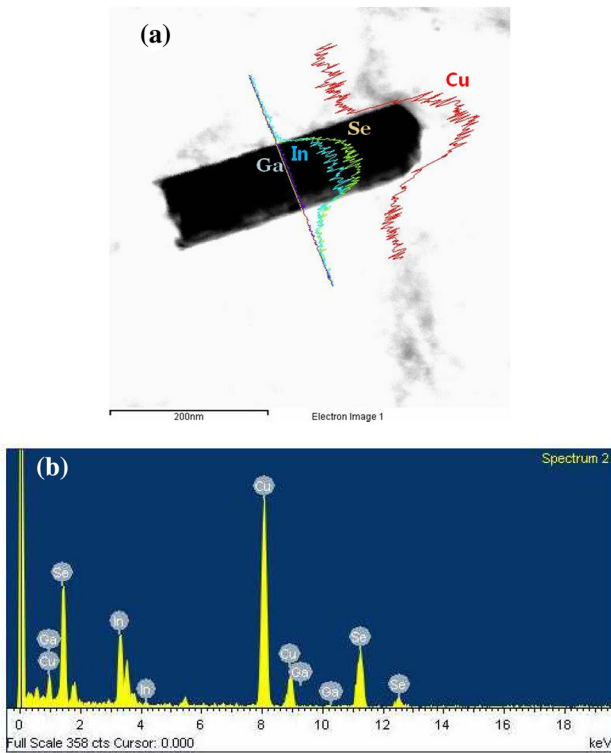
Fig. 10 TEM-based Line EDS scan (**a**) and EDS spectrum (**b**)

Table 1 Result of CIGS nanowire from EDS on the Cu grid

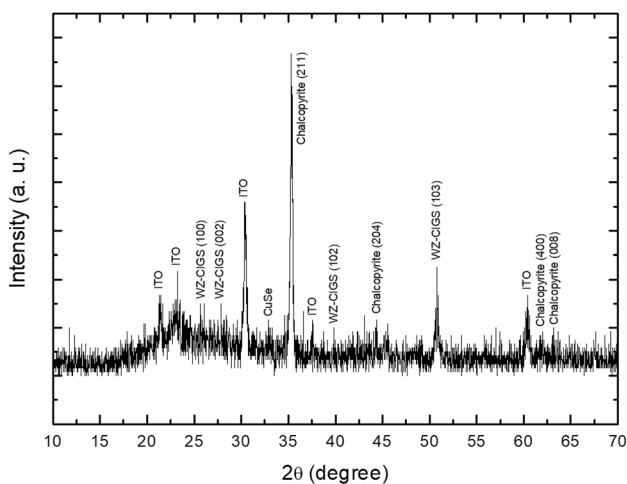| Element	wt%	at%
Cu	48.40	58.71
In	29.81	21.12
Ga	0.15	0.17
Se	21.63	20.01

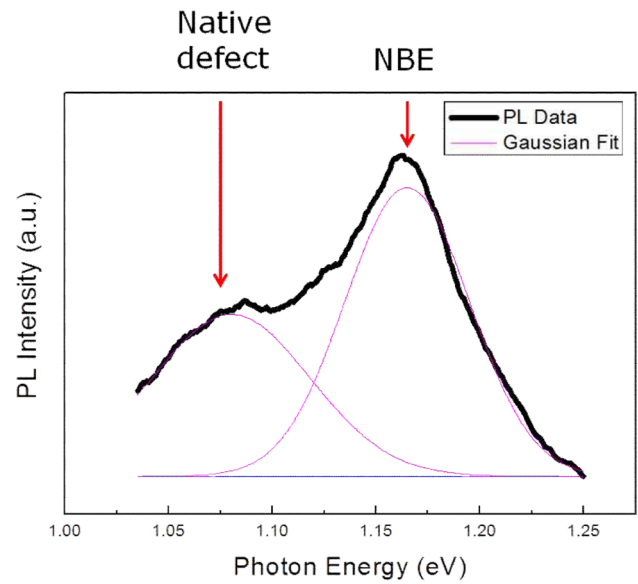**Fig. 11** XRD pattern of CIGS nanowires

Fig. 12 PL spectrum of CIGS nanowires

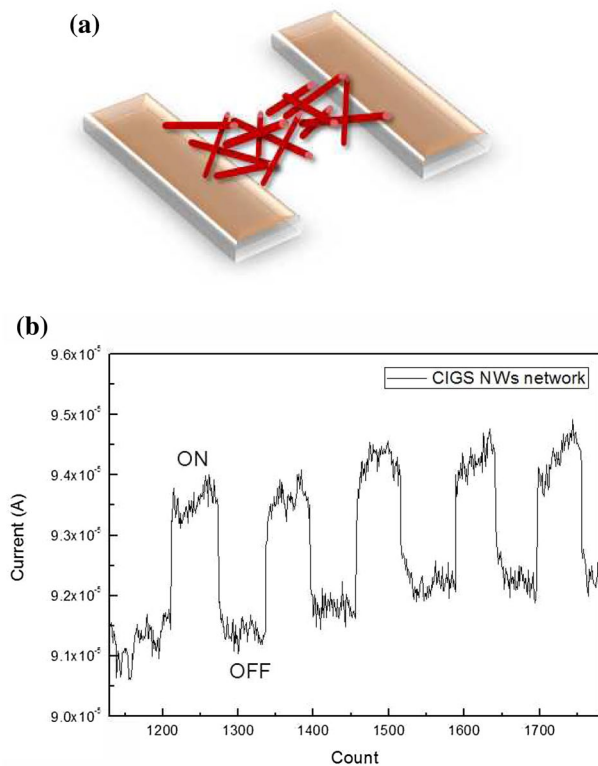**Fig. 13** **a** Schematic image of CIGS nanowire network. **b** Optical response of CIGS nanowire network

substrate because the vaporized Indium was deposited on the ITO substrate uniformly and acted as a self-catalyst. When a catalyst was used, the CIGS nanowires were grown only by using Indium. When Gallium and Gold were used,

no nanowires were present. In a catalyst environment, the length and diameter of the nanowires decreased but the density dramatically increased. TEM-based EDS indicates that the nanowires are made up of CIGS material with a very low amount of Ga. XRD measurements show the formation of wurtzite-structured CIS nanowires with a missing Ga phase. PL spectroscopy shows that near-band-edge emission occurs at 1.16 eV by band-to-band transition. Optical response of the CIGS nanowire network indicates that CIGS nanowires show appreciable photosensitivity which will definitely be useful for window solar cells and bifacial solar cell applications. Solar cell efficiency will enhance due to the increase of photon absorption by the increased surface area. The surface area increases due to increased density of crystalline nanowires. The reflectance of the substrate decreases due to growth on a transparent ITO substrate.

Compliance with ethical standards

Conflict of interest There are no conflicts of interest to declare.

References

Cheyssac P et al (2006) Vapor-liquid-solid mechanisms: challenges for nanosized quantum cluster/dot/wire materials. J Appl Phys 100:044315

Chu VB, Cho JW, Park SJ, Hwang YJ, Park HK, Do YR, Min BK (2014) Fabrication of solution processed 3D nanostructured CuInGaS2 thin film solar cells. Nanotechnology 25:125401

Cui Y et al (2007) Low temperature CO oxidation over unsupported nanoporous gold. J Am Chem Soc 129:42–43

Garnett E et al (2008) Silicon nanowire radial p–n junction solar cells. J Am Chem Soc 130:9224–9225

Heo K et al (2008) Large-scale assembly of silicon nanowire network-based devices using conventional microfabrication facilities. Nano Lett 8:4523–4527

Ho CH et al (2012) An efficient light-harvesting scheme using SiO2 nanorods for InGaN multiple quantum well solar cells. Sol Energy Mater Sol Cells 103:194–198

Huang MH et al (2001) Catalytic Growth of Zinc Oxide Nanowires by Vapor Transport. Adv Mater 13:113–116

Lee JY, Seong WK, Kim J-H, Cho S-H, Park J-K, Lee K-R, Moon M-W, Yang C-W (2015) Synthesis and characterization of single-crystal Cu(In, Ga)Se2 nanowires: high Ga contents and growth behavior. Cryst Eng Comm 17:4950

Liu C et al (2011) Large scale single-crystal Cu(In, Ga)Se2 nanotip arrays for high efficiency solar cell. Nano Lett 11:4443–4448

McEvoy A, Markvart T, Castaner L (2012) Practical handbook of photovoltaics: fundamentals and applications. Elsevier Ltd, UK, pp 7–12

Mehta BR et al (2005) A graded diameter and oriented nanorod-thin film structure for solar cell application: a device proposal. Sol Energy Mater Sol Cells 85:107–113

Moon SH, Park SJ, Hwang YJ, Lee DK, Cho Y, Kim DW, Min BK (2014) Printable, wide band-gap chalcopyrite thin films for power generating window applications. Sci Rep 4(4):4408

Norako ME, Brutchey RL (2010) Synthesis of metastable wurtzite CuInSe2 nanocrystals. Chem Mater 22:1613–1615

Shirakata S et al (2011) Near-band-edge photoluminescence in Cu(In, Ga)Se2 solar cells. Sol Energy Mater Sol Cells 95:219–222

Shirakata S et al (2012) Characterization of Cu(In, Ga)Se2 solar cell fabrication process by photoluminescence. Jpn J Appl Phys 51:10NC13

Stelzner T et al (2008) Silicon nanowire-based solar cells. Nanotechnology 19:295203

Wada T et al (2001) High-efficiency CIGS solar cells with modified CIGS surface. Sol Energy Mater Sol Cells 67:305–310

Wagner RS, Ellis WC (1964) Vapor–liquid–solid mechanism of single crystal growth. Appl Phys Lett 4:89–90

Zhang J et al (2012) CuInSe2 nanocrystals/CdS quantum dots/ZnO nanowire arrays heterojunction for photovoltaic applications. Sol Energy Mater Sol Cells 103:30–34

Publisher's Note Springer Nature remains neutral with regard to jurisdictional claims in published maps and institutional affiliations.